Physica B 480 (2016) 58–62

Contents lists available at ScienceDirect

Physica B

journal homepage: www.elsevier.com/locate/physb

Analysis of temperature-dependant current–voltage characteristics and extraction of series resistance in Pd/ZnO Schottky barrier diodes

M A Mayimele *, J P. Janse van Rensburg, F D Auret, M Diale

Department of Physics, University of Pretoria, Pretoria 0002, South Africa

ARTICLE INFO

Article history:
Received 15 May 2015
Received in revised form
29 July 2015
Accepted 31 July 2015
Available online 1 August 2015

Keywords:
Series resistance
Barrier inhomogeneities
Gaussian distribution & Modified Richardson plot

ABSTRACT

We report on the analysis of current voltage (*I–V*) measurements performed on Pd/ZnO Schottky barrier diodes (SBDs) in the 80–320 K temperature range. Assuming thermionic emission (TE) theory, the forward bias *I–V* characteristics were analysed to extract Pd/ZnO Schottky diode parameters. Comparing Cheung's method in the extraction of the series resistance with Ohm's law, it was observed that at lower temperatures (T < 180 K) the series resistance decreased with increasing temperature, the absolute minimum was reached near 180 K and increases linearly with temperature at high temperatures (T > 200 K). The barrier height and the ideality factor decreased and increased, respectively, with decrease in temperature, attributed to the existence of barrier height inhomogeneity. Such inhomogeneity was explained based on TE with the assumption of Gaussian distribution of barrier heights with a mean barrier height of 0.99 eV and a standard deviation of 0.02 eV. A mean barrier height of 0.11 eV and Richardson constant value of 37 A cm^{-2} K^{-2} were determined from the modified Richardson plot that considers the Gaussian distribution of barrier heights.

1. Introduction

In realizing semiconductor-based devices, there are various parameters that need to be taken into consideration: surface preparation process, the formation of barrier height between the metal and semiconductor and its homogeneity, density of interface states and dislocations, applied voltage and series resistance (R_s) [1,2]. Amongst all these, the R_s is an important parameter, which causes the electrical characteristics of devices to be non-ideal [3]. There are various techniques to evaluate the main electrical parameters from the forward bias *I–V* measurements such as Cheung and Cheung's method and the Ohm's law [4]. Cheung and Cheung's method brings an alternative approach from Ohm's law to determine the barrier height, ideality factor and R_s from the forward *I–V* measurements, which are the main electrical parameters in the characterisation of a SBDs and provide useful information concerning the nature of the diodes [5].

Analysis of the forward biased *I–V* characteristics of these devices only at room temperature does not give a detailed description about the current conduction mechanism. The investigation of the forward bias *I–V* characteristics in a wide temperature range gives a clear understanding of the aspects of the current transport mechanism and the barrier formation. In general, the forward bias *I–V* characteristics of these devices deviate from the ideal TE theory [6]. There is still some difficulty in predicting the exact transport phenomenon. A careful analysis of the *I–V* characteristics of the SBDs at different temperatures provides detailed information of the conduction process and the nature of the barrier formation at the metal-semiconductor interface [7]. However, in the case of inhomogeneous barrier potential between metal and semiconductor, the structure's barrier potential is resembled to a barrier consisting of higher and lower patches from which current pass through. Thus, it is possible to explain it through TE theory with the Gaussian distribution of the barrier potential [8].

In this study, we analyse temperature dependant forward biased *I–V* measurements on Pd/ZnO SBDs in the 80–320 K temperature range. The series resistance, Schottky Barrier height and ideality factors were calculated using conventional methods as well as alternative methods. Fair correlation is obtained with the alternative methods and the conventional methods in certain areas of the plots. The deviation from ideal TE transport mechanism is been an issue with ZnO materials. Hence, the TE theory with the Gaussian distribution of the barrier potential is used to explain the current transport mechanisms and the determination of the Richardson constant.

2. Experiment

In this study, undoped ZnO samples from Cermet Inc. were

* Corresponding author.
E-mail address: meehleketo@gmail.com (M. Mayimele).

http://dx.doi.org/10.1016/j.physb.2015.07.034
0921-4526/

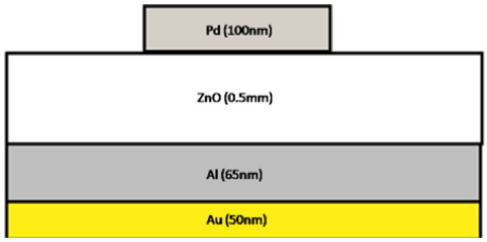

Fig. 1. A schematic diagram of Pd/ZnO SBDs.

used [9]. The samples were degreased in acetone, then methanol for five minutes each in an ultra-sonic bath. They were annealed in nitrogen gas at 800 °C for 30 min and they were again degreased in acetone and methanol. Then etched in 100 °C boiling hydrogen peroxide for three minutes and blown dry with nitrogen gas. Ohmic contacts with composition of Al/Au and relative thicknesses of 65/50 nm were deposited on the Zn polar face using the resistive evaporation technique at a pressure of approximately 1×10^{-6} Torr. Pd Schottky contacts of diameter 0.6 mm and thickness of 100 nm were fabricated on the O-polar face of the ZnO samples using the resistive evaporation system under a vacuum of approximately 1×10^{-6} Torr. Fig. 1 shows the schematic diagram of Pd/ZnO SBDs. Temperature-dependant *I–V* measurements were performed in a closed cycle Helium cryostat in the 80–320 K temperature range.

3. Results and discussion

The current–voltage (*I–V*) characteristics of Pd/ZnO Schottky barrier diodes in the 80–320 K temperature range are plotted in Fig. 2(a). The behaviour of the curves shows strong temperature dependence and a deviation from the ideal Schottky barrier diodes. Assuming standard thermionic emission (TE) theory, the barrier height (Φbo) and ideality factor (n) are extracted using Eqs. (1) and (2) and a linear fit to the *I–V* data [10].

$$\Phi_{bo} = \frac{kT}{q} ln\left[\frac{AA^*T^2}{I_s}\right] \tag{1}$$

and

$$n = \frac{q}{kT}\left(\frac{dV}{dlnI}\right) \tag{2}$$

where I_s is the saturation current, k is the Boltzmann constant, q is the electronic charge, T is temperature in Kelvin, A is the diode area in square centimetres, Φ_{bo} is barrier height in eV and A^* is the Richardson constant, evaluated at 32 A cm^{-2} K^{-2} for n-ZnO [2].

From Eqs. (1) and (2) the values of Φ_{bo} and n of the Pd/ZnO in the 80–320 K temperature range are plotted in Fig. 2(b). The behaviour of the curves show that the Φ_{bo} increases and the n decreases with increasing temperature. This explains the deviation of the *I–V* characteristics from the pure TE mechanism, in which the Φ_{bo} and the n should remain constant with temperature. The higher values of n can be attributed to the presence of barrier height inhomogeneities at the interface, minority carrier injections, the image force effect and the formation of a particular distribution state at the semiconductor band gap [11]. Several researchers [8,12] reported a similar behaviour of the barrier height, which disagree with the negative temperature coefficient of resistance in II–IV metal-semiconductors (MS). Another possible explanation of the observed behaviour is the temperature-activated current transport of charge carriers across the MS interface [13]. At low temperatures, electrons are able to surmount the lower barrier through tunnelling [8]. Therefore, tunnelling will be the dominant transport mechanism of charge carriers through the patches at lower Φ_{bo}. As temperature increase, more electrons access sufficient energy to surmount the barrier height areas through TE, explaining the behaviour of barrier height increasing with increasing temperature [14].

From Fig. 2(a) the forward bias current voltage (*I–V*) characteristics are linear on the semilogarithmic scale from 0.0 V to 0.5 V then deviate due to R_s. Hence, it is of vital importance to determine the R_s using a variety of methods. The simplest way to determine the R_s values is Ohm's law, which yields R_s as dV/dI in the forward bias region and another way of determining the R_s is by Cheung and Cheung's method [1,3]. The forward bias *I–V* characteristics due to TE theory of Schottky diodes with the R_s can be expressed as Cheung's functions [4]:

$$\frac{dV}{d(\ln I)} = IR_s + n\left(\frac{kT}{q}\right) \tag{3}$$

and

$$H(I) = V - n\left(\frac{kT}{q}\right)ln\left(\frac{I}{AA^*T^2}\right) = n\Phi_{bo} + IR_s \tag{4}$$

From Fig. 3(a), the plot is linear with R_s as the gradient and $n\Phi_{bo}$ as the y-axis intercepts derived from Eq. (3). The insert in Fig. 3 (a) shows a plot of the whole range of the forward bias *I–V* data, which can be divided into two regions. In region I, the ideality factor is similar to that obtained using ohm's law, with high values of R_s, where the R_s determined from region II are in good agreement with those of obtained from the *I–V* curves. The observed behaviour can be attributed to the existence of the R_s, interface states and to the voltage drop across the interfacial layers.

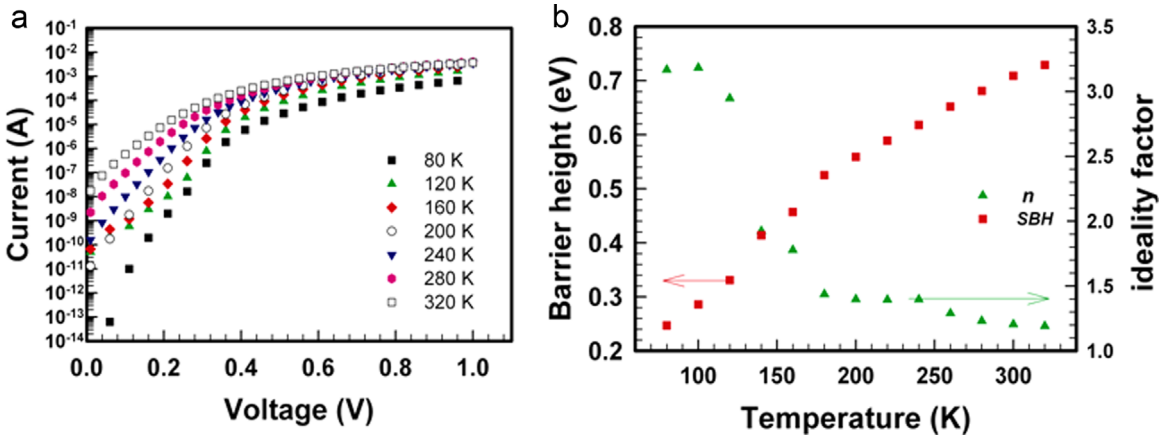

Fig. 2. (a) Semi logarithmic forward current–voltage (*IV*) characteristics, (b) barrier height and ideality factor as a function of temperature for Pd/ZnO SBDs.

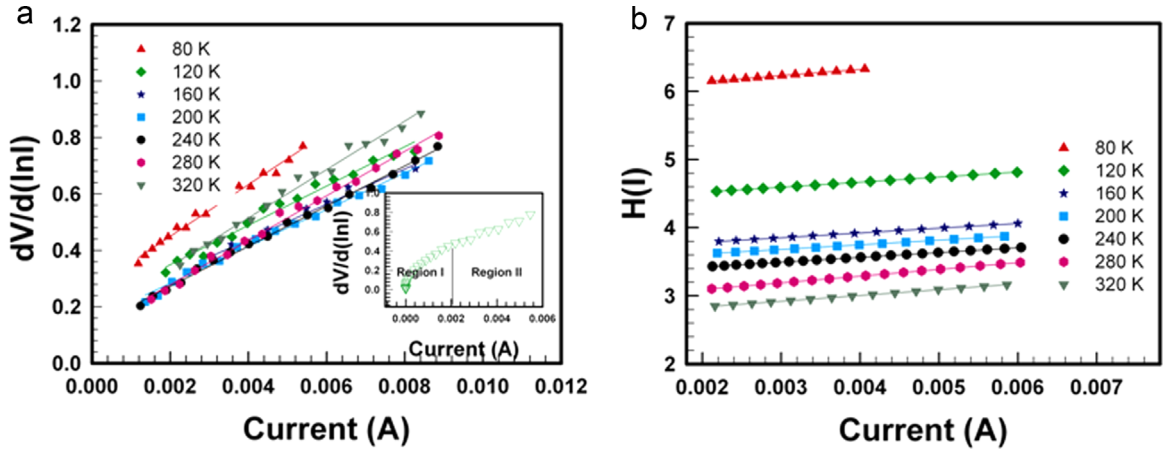

Fig. 3. (a) & (b) Cheung and Cheung's functions against the forward current characteristics of Pd/ZnO SBDs.

Furthermore, the plot of H(I)-I is linear, with the gradient of this plot providing a different determination of R_s. Thus, by using the value of the n obtained from Eq. (3) the value of Φ_{bo} can be calculated from the y-axis intercept of the H(I)-I plot. Similar observations were reported by Durmus et al. [15] on Au/n-Si SBD and Kinaci et al. [5] on Au/TiO2/n-Si SDB.

The R_s obtained from the three different techniques were plotted in Fig. 4(a). Mtangi et al [16] observed a similar trend of series resistance obtained from lnI-V plots on Pd/ZnO SBD in the 60–300 K temperature range. They explained the observed trend to be related to bulk resistivity of the sample determined from the Hall effect measurements, where a transition in the conductivity occurs near 180 K. From Fig. 4(a) shows that at lower temperatures ($T < 180$ K), the R_s decreases with increase in temperatures, while showing an absolute minimum near 180 K and increases linearly with temperature at high temperatures ($T > 200$ K).

As discussed earlier, temperature influences Φ_{bo} (Fig. 2(b)). Another way of determining the Φ_{bo} and the Richardson constant in a range of temperatures, Eq. (1) can be rewritten as,

$$ln\left(\frac{I_s}{T^2}\right) = ln(AA^*) - \frac{q\Phi_{bo}}{kT} \tag{5}$$

Fig. 4(b) shows a plot of the conventional energy variation of ln (I_s/T^2) against $10^3/T$ in the 180-320 K temperature range. Although the entire study of temperature dependant *I-V* measurements were conducted in the 80–320 K temperature range, a non-linear behaviour was observed at lower temperatures. Hence, linear region of 180–320 K was plotted in Fig. 4(b). The non-linearity of the plot can be attributed to the dependence of the barrier height and the ideality factor on temperature. The Φ_{bo} and Richardson constant were determined from the gradient and the y-axis intercept in Fig. 4(b), respectively. The Richardson constant was determined as 3×10^{-9} A cm^{-2} K^{-2} in the180–320 K temperature range. These values are much lower compared to the theoretical value of 32 A cm^{-2} K^{-2} in n-ZnO. The effective barrier height is 0.26 eV in the 180–320 K temperature range. The deviation in the Richardson plot may be due to the presence of the spatially inhomogeneous barrier height and the potential fluctuations at the interface that consists of low and high barrier areas, i.e. when the temperature is lowered, the current will flow preferentially through the lower barriers in the potential distribution [17–19].

An analytical potential fluctuation method on spatially inhomogeneous SBD can be used to quantitatively explain the non-ideal *I–V* behaviour of Pd/ZnO Schottky diode, by assuming the Gaussian distribution of the SBH with the mean value of SBH ($\overline{\Phi}_{bo}(T=0)$) and a standard deviation (σ_{so}) of the SBH distribution. The total current in a given forward bias V is then given by

$$I = I_s \exp\left(\frac{qV}{n_{ap}kT}\right)\left[1 - exp\left(\frac{-qV}{kT}\right)\right] \tag{6}$$

with

$$I_s = AA^*T^2\exp\left(\frac{q\Phi_{ap}}{kT}\right), \tag{7}$$

Where n_{ap} and Φ_{ap} are the apparent ideality factor and apparent Schottky barrier height, respectively, given by [17]

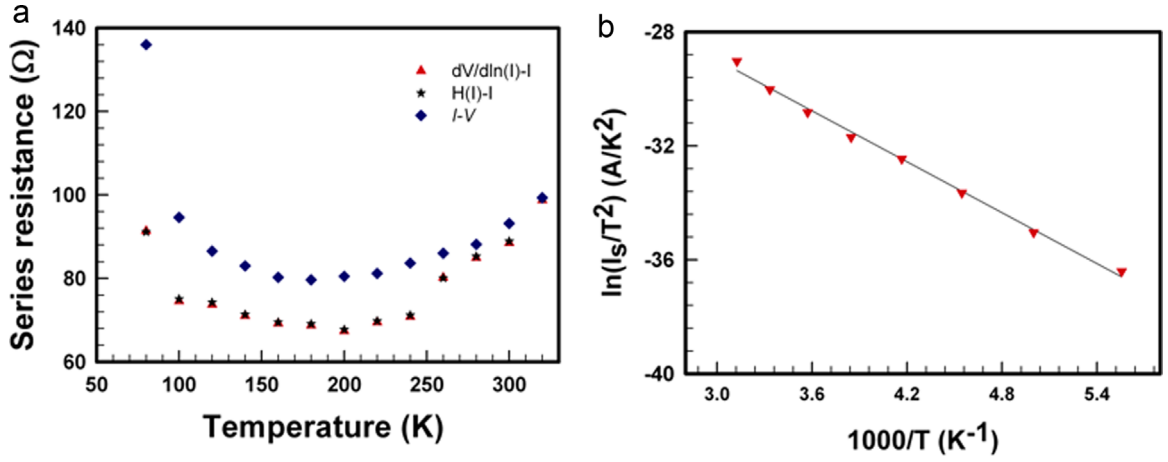

Fig. 4. (a) Series resistance as a function of temperature using 3 different methods and (b) Richardson plot, $ln\ (I_s/T^2)$ versus 1000/T for Pd/ZnO SBDs.

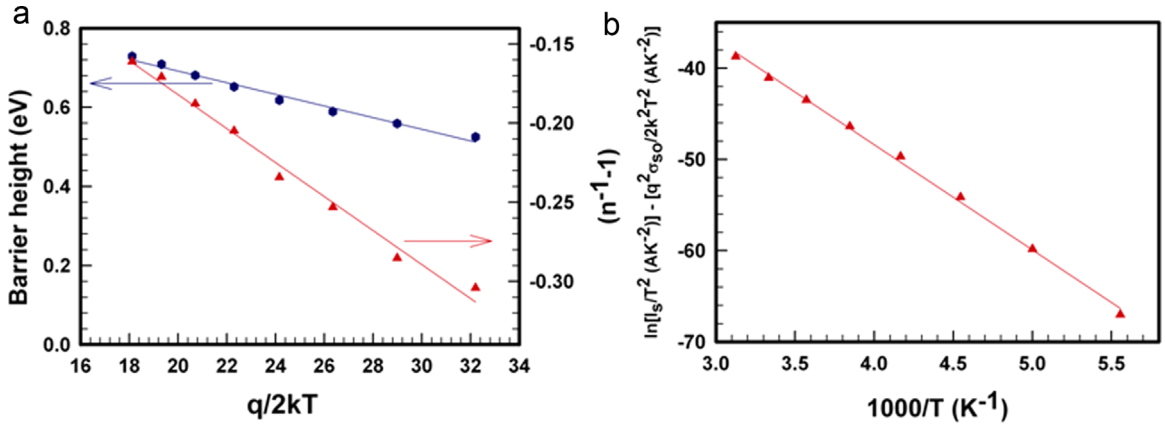

Fig. 5. (a) Zero-bias apparent barrier height and the inverse ideality factor versus *q/2kT* and (b) Modified Richardson plot for the Pd/ZnO SBDs according to the Gaussian distribution of the barrier heights.

$$\Phi_{ap} = \overline{\Phi}_{bo}(T=0) - \frac{q\sigma_{so}^2}{2kT} \tag{8}$$

$$\left(\frac{1}{n_{ap}} - 1\right) = -\rho_2 + \frac{q\rho_3}{2kT} \tag{9}$$

Here ρ_2 and ρ_3 are voltage coefficients, which may depend on temperature, used to quantify the voltage deformation of the SBH distribution [20]. Fig. 5(a) shows a linear plot of barrier height vs. $q/2kT$, ($\overline{\Phi}_{bo}(T=0)$) and σ_{so}, which were extracted using Eq. (8) as the *y*-axis intercept and the gradient obtained as 0.99 eV and 0.02 V, respectively. The smaller the value of the σ_{so}, the more homogeneous the barrier height is and the better the diode. A linear plot of ideality factor vs. *q/2kT*, using Eq. (9) shown in Fig. 4 (a) gives the voltage coefficients ρ_2 and ρ_3 as the intercepts and gradient, respectively, are obtained as 0.03 and −0.01 eV, respectively. The linear behaviour of the plot shows that the ideality factor expresses the voltage deformation of the Gaussian distribution of the SBD.

The Richardson constant extracted from the conventional activation energy $ln(I_s/T^2)$ vs. 1000/*T* plot was much lower than the theoretical value due to the lateral inhomogeneity of the Schottky barrier. A more reliable value of the Richardson constant can be determined using modified Arrhenius plot by eliminating the effect of the inhomogeneity. A modified expression according to the Gaussian distribution of the SBHs can be obtained by using Eqs. (8) and (9) in Eq. (5) as

$$\ln\left(\frac{I_s}{T^2}\right) - \left(\frac{q^2\sigma_o^2}{2k^2T^2}\right) = ln(AA^{**}) - \left[\frac{q\Phi_{bo}}{kT}\right] \tag{10}$$

The modified $ln(I_s/T^2) - (q^2\sigma_o^2)/(2k^2T^2)$ vs. 1000/T plot shown in Fig. 5(b) should yield a straight line following the Eq. (10) with the gradient directly yielding the mean Φ_{bo} and the intercept at the y-axis yielding the modified Richardson constant (A^{**}). The values of $ln(I_s/T^2) - (q^2\sigma_o^2)/(2k^2T^2)$ were calculated using the value of σ_{so}. From the plot, the mean Φ_{bo} and A^{**} were determined to be 0.99 eV and 37 A cm^{-2} K^{-2} without using the temperature coefficients of the barrier heights, respectively. The mean Φ_{bo} extracted using the modified Richardson plot was identical to 0.99 eV obtained from the plot of barrier height vs. *q/2kT* as shown in Fig. 5(a). Furthermore, the modified Richardson constant of 37 A cm^{-2} K^{-2} is very close to the theoretical value of n-ZnO of 32 A cm^{-2} K^{-2}, implying the validity of the analytical model predicting the Gaussian type of the barrier height distribution in Pd/ZnO Schottky diode.

4. Conclusion

Analysis of the forward bias *I–V* measurements of Pd/ZnO Schottky barrier diodes were investigated in a wide temperature range of 80–320 K. The series resistance obtained in this study are in good agreement with literature and with each other. The current transport mechanism at lower temperature is dominated by the current flow through the low Schottky barrier areas and tunnelling. Meanwhile at high temperatures, TE is the dominant current transport mechanism. Barrier height and the ideality factor decreased and increased, respectively, with decreasing temperature, attributed to the existence of barrier height inhomogeneity. Such inhomogeneity has been successfully explained based on TE with the assumption of Gaussian distribution of barrier heights with a mean barrier height of 0.986 eV and a standard deviation of 0.015 V. A mean barrier height of 0.994 eV and Richardson constant value of 37 A cm^{-2} K^{-2} were determined from the modified Richardson plot that considers the Gaussian distribution of barrier heights.

Acknowledgement

The South Africa National Research Foundation (NRF) and the University of Pretoria for financial support.

References

[1] F.Z. Pür, A. Tataroğlu, Phys. Scr. 86 (2012) 035802.
[2] Ü. Özgür, Y.I. Alivov, C. Liu, A. Teke, M.A. Reshchikov, S. Doğan, V. Avrutin, S.-J. Cho, H. Morkoç, J. Appl. Phys. 98 (2005) 041301–041301-103.
[3] Z. Ahmad, M.H. Sayyad, Physica E 41 (2009) 631–634.
[4] S.K. Cheung, N.W. Cheung, Appl. Phys. Lett. 49 (1986) 85–87.
[5] B. Kinaci, T. Asar, Y. Özen, S. Özçelik, Optoelectron. Adv. Mater. Rapid Commun. 5 (2011) 434–437.
[6] E. Gür, S. Tüzemen, B. Kiliç, C. Coşkun, J. Phys. Condens. Matter (2007) 196–206.
[7] J.-Y. Jeong, V. Janardhanam, H.-J. Yun, J.-H. Lee, J.-Y. Kim, K.-H. Shim, C.-J. Choi, Jap. J. Appl. Phys. 53 (2014) 08NH01.
[8] H. Tecimer, A. Türüt, H. Uslu, Ş. Altındal, İ. Uslu, Sens. Actuators A: Phys. 199 (2013) 194–201.
[9] http://www.cermetinc.com/materials/n__ZnO_substrate_product_lit.2014.
[10] S. Sze, K.K. Ng, Physics of Semiconductor Devices: Third Edition, 2006.
[11] D. Korucu, T.S. Mammadov, J. Optoelectron. Adv. Mater. 14 (2012) 41–48.
[12] B.G. Yacobi, Semiconductor Materials, An Introduction to Basic Principles, Springer, US, 2013.
[13] M.A. Mayimele, M. Diale, W. Mtangi, F.D. Auret, Mater. Sci. Semicond. Process. 34 (2015) 359–364.
[14] I. Hussain, M. Soomro, N. Bano, O. Nur, M. Willander, J. Appl. Phys. 113 (2013) 234509.
[15] P. Durmuş, M. Yıldırım, Mater. Sci. Semicond. Process. 27 (2014) 145–149.

[16] W. Mtangi, Electrical Characterization of ZnO and Metal ZnO Contacts, University of Pretoria, South Africa, 2009.
[17] A. Özdemir, A. Turut, A. Kökçe, Semicond. Sci. Technol. 21 (2006) 298.
[18] S.M. Faraz, V. Khranovskyy, R. Yakimova, A. Ulyashin, Q. Wahab, IEEE Regional Symposium on Micro and Nanoelectronics (RSM), 2011, 48–51.
[19] H. Asil, K. Çinar, E. Gür, C. Coşkun, S. Tüzemen, Int. J. 8 (2013) 371–379.
[20] E. Özavcı, S. Demirezen, U. Aydemir, Ş. Altindal, Sens. Actuators A Phys. 194 (2013) 259–268.